ISSN 1674-1056
http://cpb.iphy.ac.cn
http://iopscience.iop.org/cpb
中国物理 B
Chinese Physics
中国物理 Chinese Physics B

Nodeless superconductivity in a quasi-two-dimensional superconductor $AuTe_2Se^{4/3}$

Xiao-Yu Jia(贾小雨), Yun-Jie Yu(俞云杰), Xu Chen(陈旭), Jian-Gang Guo(郭建刚), Tian-Ping Ying(应天平), Lan-Po He(何兰坡), Xiao-Long Chen(陈小龙), Shi-Yan Li(李世燕)
Citation: Chin. Phys. B . 2018, 27(6): 067401. **doi:** 10.1088/1674-1056/27/6/067401

Journal homepage: http://cpb.iphy.ac.cn; http://iopscience.iop.org/cpb

What follows is a list of articles you may be interested in

Superconductivity in self-flux-synthesized single crystalline $R_2Pt_3Ge_5$(*R* = La, Ce, Pr)

Q Sheng(盛琪), J Zhang(张建), K Huang(黄百畅), Z Ding(丁兆峰), X Peng(彭小冉), C Tan(谭程), L Shu(殳蕾)
Chin. Phys. B . 2017, 26(5): 057401. **doi:** 10.1088/1674-1056/26/5/057401

Multiband nodeless superconductivity near the charge-density-wave quantum critical point in $ZrTe_{3-x}Se_x$

Shan Cui(崔珊), Lan-Po He(何兰坡), Xiao-Chen Hong(洪晓晨), Xiang-De Zhu(朱相德), Cedomir Petrovic, Shi-Yan Li(李世燕)
Chin. Phys. B . 2016, 25(7): 077403. **doi:** 10.1088/1674-1056/25/7/077403

High-pressure studies on heavy fermion systems

Ye Chen(陈晔), Zongfa Weng(翁宗法), Smidman Michael, Xin Lu(路欣), Huiqiu Yuan(袁辉球)
Chin. Phys. B . 2016, 25(7): 077401. **doi:** 10.1088/1674-1056/25/7/077401

Superconductivity in Sm-doped $CaFe_2As_2$ single crystals

Dong-Yun Chen(陈东云), Bin-Bin Ruan(阮彬彬), Jia Yu(于佳), Qi Guo(郭琦), Xiao-Chuan Wang(王小川), Qing-Ge Mu(穆青隔), Bo-Jin Pan(潘伯津), Tong Liu(刘通), Gen-Fu Chen(陈根富), Zhi-An Ren(任治安)
Chin. Phys. B . 2016, 25(6): 067403. **doi:** 10.1088/1674-1056/25/6/067403

Effect of residual stress on nematic domains in $BaFe_{2-x}Ni_xAs_2$ studied by angular magnetoresistance

Ding Hu(胡定), Wenliang Zhang(张汶良), Yuan Wei(魏源), Xiaotian Zhang(张笑天), Cong Ren(任聪), Lei Shan(单磊), Yi-feng Yang(杨义峰), Huiqian Luo(罗会仟), Shiliang Li(李世亮)
Chin. Phys. B . 2016, 25(5): 057402. **doi:** 10.1088/1674-1056/25/5/057402

RAPID COMMUNICATION

Nodeless superconductivity in a quasi-two-dimensional superconductor $AuTe_2Se_{4/3}$*

Xiao-Yu Jia(贾小雨)[1], Yun-Jie Yu(俞云杰)[1], Xu Chen(陈旭)[2], Jian-Gang Guo(郭建刚)[2], Tian-Ping Ying(应天平)[1], Lan-Po He(何兰坡)[1], Xiao-Long Chen(陈小龙)[2,3,4], and Shi-Yan Li(李世燕)[1,5,†]

[1] *State Key Laboratory of Surface Physics, Department of Physics, and Laboratory of Advanced Materials, Fudan University, Shanghai* 200433, *China*
[2] *Beijing National Laboratory for Condensed Matter Physics, Institute of Physics, Chinese Academy of Sciences, Beijing* 100190, *China*
[3] *School of Physical Sciences, University of Chinese Academy of Sciences, Beijing* 100049, *China*
[4] *Collaborative Innovation Center of Quantum Matter, Beijing* 100084, *China*
[5] *Collaborative Innovation Center of Advanced Microstructures, Nanjing* 210093, *China*

(Received 16 April 2018; revised manuscript received 24 April 2018; published online 30 May 2018)

We performed ultra-low temperature thermal conductivity measurements on the single crystal of a new gold-based quasi-two-dimensional superconductor $AuTe_2Se_{4/3}$, which has a superconducting transition temperature $T_c = 2.70$ K. A negligible residual linear term κ_0/T in zero magnetic field is observed, which suggests fully gapped superconducting state. Furthermore, the field dependence of κ_0/T is similar to that of the multi-band s-wave superconductor $BaFe_{1.9}Ni_{0.1}As_2$ at low field. These results reveal multiple nodeless superconducting gaps in this interesting quasi-two-dimensional superconductor with Berezinsky–Kosterlitz–Thouless topological transition.

Keywords: superconductivity, thermal transport measurement, gap structure, two-dimensional material

PACS: 74.25.fc, 74.25.Jb, 74.25.Op, 74.70.Dd **DOI:** 10.1088/1674-1056/27/6/067401

1. Introduction

Two-dimensional (2D) superconductivity has been extensively studied in recent years to explore exotic quantum phenomena, such as high-temperature superconductivity and various quantum phase transitions.[1–3] There are several ways to realize the 2D superconductivity as described below.

(i) It can be realized in ultra-thin films grown by molecular beam epitaxy method, e.g., in monolayer FeSe/$SrTiO_3$ ($T_c = 65$ K),[1] ultra-thin Ga films ($T_c^{zero} \approx 3.62$ K),[2] and highly crystalline Pb thin films ($T_c = 1.5$ K).[4,5]

(ii) The 2D superconductivity can be found in some particular interfaces or surfaces, e.g., the $LaAlO_3/SrTiO_3$ interface ($T_c = 0.2$ K),[6] the interface of an insulator and a metal $La_2CuO_4/La_{1.55}Sr_{0.45}CuO_4$ (T_c exceeds 50 K),[7] and the surface of MoS_2 thin flake by ionic liquid gating (the maximum $T_c = 10.8$ K).[8,9]

(iii) By vertically putting two graphene sheets together with certain twisted angles, both a Mott-like insulating state and a superconducting state ($T_c \approx 1.7$ K) arise from the electrons localized in these 2D superlattices.[10,11]

(iv) An relatively easier way is to mechanically exfoliate thin flakes directly from bulk van der Waals (vdW) quasi-2D superconductors. $Bi_2Sr_2CaCu_2O_{8+x}$ (Bi-2212) and $NbSe_2$ have been successfully cleaved to atomic thin sheets with different thicknesses, in which superconductivity has been observed ($T_c = 82$ K for half-unit-cell Bi-2212 and $T_c = 3.1$ K for monolayer $NbSe_2$, respectively).[12–15] In this context, it is important to find more attractive vdW quasi-2D superconductors.

Very recently, a new gold-based quasi-2D superconductor $AuTe_2Se_{4/3}$ has been discovered.[16] Despite that metastable $Au_{1-x}Te_x$ ($0.6 < x < 0.85$) compounds are superconductors with T_c between 1.5 K and 3.0 K,[17,18] calaverite $AuTe_2$ is a non-superconducting compound.[19] By introducing Se atoms into $AuTe_2$, electrons from Te have been attracted by the Se anions, and superconductivity with $T_c^{onset} = 2.85$ K was found in $AuTe_2Se_{4/3}$.[16] Furthermore, it manifests the 2D Berezinsky–Kosterlitz–Thouless (BKT) topological transition based on the measurements of standard I–V curves around T_c, which indicates the superconductivity is mainly confined in the *ab* plane.[16] This is consistent with the fact that the interaction of interlayer is Van der Waals force in $AuTe_2Se_{4/3}$, and the $AuTe_2Se_{4/3}$ single crystal can be very easily exfoliated into thin flakes by Scotch tape.[16] Therefore, $AuTe_2Se_{4/3}$ is a new vdW quasi-2D superconductor.

To understand the superconducting pairing mechanism of

*Project supported by the Key Basic Research Program of China (Grant Nos. 2015CB921401 and 2016YFA0300503), the National Natural Science Foundation of China (Grant Nos. 11422429 and 11421404), China Postdoctoral Science Foundation (Grant No. 2016T90332), the Program for Professor of Special Appointment (Eastern Scholar) at Shanghai Institutions of Higher Learning, and STCSM of China (Grant No. 15XD1500200), and the Strategic Priority Research Program (B) of the Chinese Academy of Sciences (Grant No. XDB04040200).

†Corresponding author. E-mail: shiyan_li@fudan.edu.cn

© 2018 Chinese Physical Society and IOP Publishing Ltd

a new superconductor, it is crucial to know the superconducting gap structure first. In this work, we measure the ultra-low-temperature thermal conductivity of $AuTe_2Se_{4/3}$ single crystal down to 100 mK, to determine its superconducting gap structure. A negligible residual linear term κ_0/T in zero field and a slow field dependence of κ_0/T at low field are revealed, which suggest multiple nodeless superconducting gaps in this interesting vdW quasi-2D superconductor. This agrees with our previous band structure calculations in Ref. [16].

2. Experiment

Single crystals of $AuTe_2Se_{4/3}$ were grown by the self-flux method.[16] The obtained single crystals have ribbon shape with shining mirror-like surfaces, as shown in the inset of Fig. 1(a). The largest surface was identified as the *ab* plane by x-ray diffraction (XRD) measurement, as shown in Fig. 1(a), in which only (00*l*) Bragg peaks show up. The sample for transport measurements was cut to a rectangular shape of 2.20 mm × 0.60 mm in the *ab* plane, with a thickness of 0.20 mm perpendicular to the *ab* plane. Four gold electrodes were fabricated on the sample by thermal evaporation to ensure a good contact at low temperature. Four silver wires were then attached to the electrodes with silver paint, which were used for both resistivity and thermal conductivity measurements, with electrical and heat currents in the *ab* plane. The contacts are metallic with typical resistance of 5 mΩ at 0.3 K. The thermal conductivity was measured in a dilution refrigerator, using two RuO_2 chip thermometers, calibrated *in situ* against a reference RuO_2 thermometer. All the magnetic fields for resistivity and thermal conductivity measurements were applied perpendicular to the *ab* plane. To ensure a homogeneous field distribution in the sample, all fields were applied at temperature above the temperature T_c.

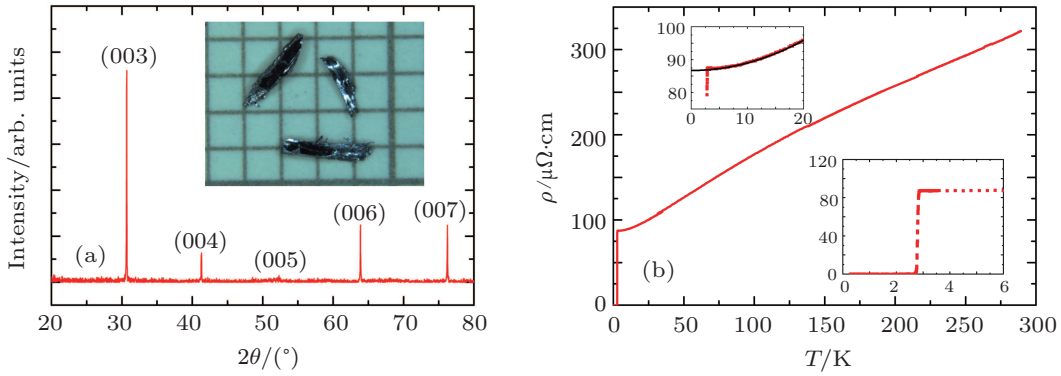


Fig. 1. (color online) (a) X-ray diffraction pattern of $AuTe_2Se_{4/3}$ single crystal. Only (00*l*) Bragg peaks show up, demonstrating that the largest surface is *ab* plane. Inset: Optical image of our $AuTe_2Se_{4/3}$ single crystals. (b) The temperature dependence of resistivity at zero field for $AuTe_2Se_{4/3}$ single crystal. Top inset: The fit of the normal-state resistivity to the Fermi-liquid behavior $\rho(T) = \rho_0 + AT^2$ from 3 K to 15 K. Bottom inset: The resistive superconducting transition at low temperature.

3. Results and discussion

Figure 1(b) shows the temperature dependence of the resistivity $\rho(T)$ for $AuTe_2Se_{4/3}$ single crystal at zero field. From the bottom inset of Fig. 1(b), the width of the resistive superconducting transition (10%–90%) is less than 0.05 K. The T_c defined by $\rho = 0$ is 2.70 K, which is consistent with our previous magnetic susceptibility measurement.[16] From 3 K to 15 K, the normal-state resistivity can be well fitted by the Fermi-liquid behavior $\rho(T) = \rho_0 + AT^2$, as shown in the top inset of Fig. 1(b). The obtained residual resistivity $\rho_0 = 87.3$ μΩ·cm gives the residual resistivity ratio (RRR) ρ (290 K)/$\rho_0 \approx 3.69$.

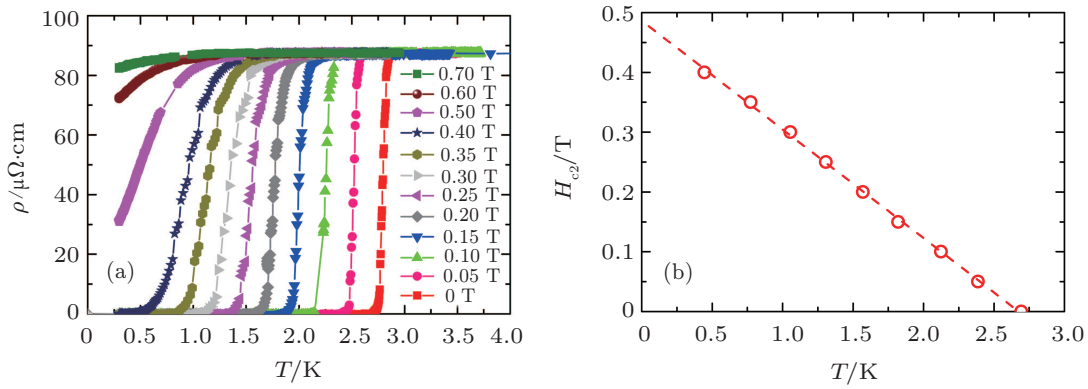


Fig. 2. (color online) (a) Low-temperature resistivity of $AuTe_2Se_{4/3}$ single crystal in magnetic fields up to 0.7 T. (b) Temperature dependence of the upper critical field $H_{c2}(T)$, defined by $\rho = 0$. The dashed line is a linear fit to the data, which points to $H_{c2}(0) \approx 0.49$ T.

In order to estimate the upper critical field $H_{c2}(0)$, the low-temperature resistivity of the $AuTe_2Se_{4/3}$ single crystal was measured in magnetic fields up to 0.7 T, as shown in Fig. 2(a). The temperature dependence of $H_{c2}(T)$, defined by $\rho = 0$, is plotted in Fig. 2(b). One can see an apparently linear temperature dependence of H_{c2}. With a linear fit to the data, $H_{c2}(0) \approx 0.49$ T is roughly estimated. Actually, the linear temperature dependence of H_{c2} in Fig. 2(b) is very interesting. It may be explained by a two-band Fermi surface topology as in MgB_2,[20–22] or an unconventional superconducting state as in heavy-fermion compound UBe_{13}.[23] Density function theory calculation shows there are four bands in $AuTe_2Se_{4/3}$,[16] therefore its linear behavior of $H_{c2}(T)$ likely originates from multiple-band Fermi surface topology.

Ultra-low temperature thermal conductivity measurement is an established bulk technique to probe the superconducting gap structure.[24] The temperature dependence of thermal conductivity for the $AuTe_2Se_{4/3}$ single crystal in zero and magnetic fields is plotted in Fig. 3. The measured thermal conductivity contains two contributions, $\kappa = \kappa_e + \kappa_p$, which come from electrons and phonons, respectively. In order to separate the two contributions, all the curves are fitted to $\kappa/T = a + bT^{\alpha-1}$ below 0.3 K.[25,26] The two terms aT and bT^{α} represent contributions from electrons and phonons, respectively. The residual linear term $\kappa_0/T \equiv a$ is obtained by extrapolating κ/T to $T = 0$ K. Due to the specular reflections of phonons at the sample surfaces, the power α in the second term is typically between 2 and 3.[25,26]

In zero field, the fitting gives $\kappa_0/T = -9.9 \pm 11$ $\mu W \cdot K^{-2} \cdot cm^{-1}$ and $\alpha = 2.41$, as seen in Fig. 3(a). Comparing with our experimental error bar ± 5 $\mu W \cdot K^{-2} \cdot cm^{-1}$, the κ_0/T of $AuTe_2Se_{4/3}$ in zero field is negligible. For s-wave nodeless superconductors, there are no fermionic quasiparticles to conduct heat in the zero-temperature limit, since all electrons form Cooper pairs.[24,25] Therefore there is no residual linear term of κ_0/T, for examples in V_3Si and $NbSe_2$.[25,27] However, for nodal superconductors, a substantial κ_0/T in zero field contributed by the nodal quasiparticles has been found.[24] For example, κ_0/T of the overdoped d-wave cuprate superconductor $Tl_2Ba_2CuO_{6+\delta}$ (Tl-2201, $T_c = 15$ K) is 1.41 $mW \cdot K^{-2} \cdot cm^{-1}$.[28] For the p-wave superconductor Sr_2RuO_4 ($T_c = 1.5$ K), $\kappa_0/T = 17$ $mW \cdot K^{-2} \cdot cm^{-1}$ was reported.[29] Therefore, the negligible κ_0/T of $AuTe_2Se_{4/3}$ strongly suggests nodeless superconducting gap in it.

In Fig. 3(b), between $H = 0$ T and 0.5 T, we fit all the curves to obtain the κ_0/T for each magnetic field. Since κ/T starts to saturate at 0.40 T, we take $H = 0.40$ T as the bulk $H_{c2}(0)$ of $AuTe_2Se_{4/3}$. This value is slightly lower than that determined by resistivity measurements in Fig. 2. Note that the choice of a slightly different $H_{c2}(0)$ does not affect our discussion on the field dependence of κ_0/T below. The obtained $\kappa_0/T = 0.28 \pm 0.004$ $mW \cdot K^{-2} \cdot cm^{-1}$ in $H_{c2}(0) = 0.40$ T meets the normal-state Wiedemann–Franz law expectation $L_0/\rho_0 = 0.28$ $mW \cdot K^{-2} \cdot cm^{-1}$ very well, with the Lorenz number $L_0 = 2.45 \times 10^{-8}$ $W \cdot \Omega \cdot K^{-2}$ and $\rho_0(0.4\ T) = 87.3$ $\mu\Omega \cdot cm$. The verification of the Wiedemann–Franz law in the normal state demonstrates that our thermal conductivity measurements are reliable.

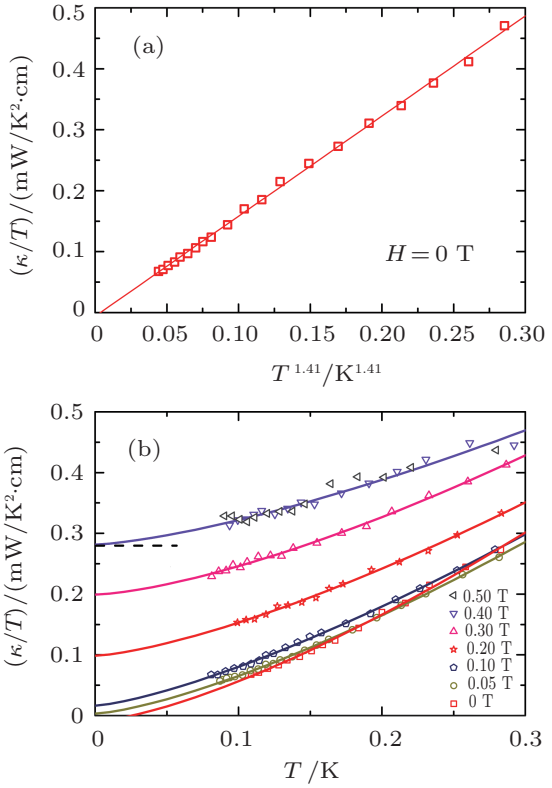


Fig. 3. (color online) Low-temperature thermal conductivity of $AuTe_2Se_{4/3}$ single crystal (a) in zero field, and (b) in magnetic fields applied perpendicular to the *ab* plane. The solid lines represent the fits to $\kappa/T = a + bT^{\alpha-1}$ for the data in different H. The dashed line is the normal-state Wiedemann–Franz law expectation $L_0/\rho_0(0.4\ T)$, with the Lorenz number $L_0 = 2.45 \times 10^{-8}$ $W \cdot \Omega \cdot K^{-2}$ and $\rho_0(0.4\ T) = 87.3$ $\mu\Omega \cdot cm$.

The field dependence of κ_0/T can provide further information on the superconducting gap structure.[24] In Fig. 4, we plot the normalized $\kappa_0(H)/T$ as a function of H/H_{c2} for $AuTe_2Se_{4/3}$. For comparison, similar data of the clean s-wave superconductor Nb,[30] the dirty s-wave superconducting alloy InBi,[31] the multiband s-wave superconductor $NbSe_2$,[27] and iron-based superconductor $BaFe_{1.9}Ni_{0.1}As_2$,[32] and an overdoped d-wave cuprate superconductor Tl-2201[28] are also plotted. For a single band s-wave superconductor Nb,[30] the $\kappa(H)/T$ changes little even up to 40% H_{c2}, while for the nodal superconductor Tl-2201, a small field can yield a quick growth in the quasiparticle density of states (DOS) due to the Volovik effect, and the low-field $\kappa_0(H)/T$ shows a roughly dependence of $\sqrt{H}$.[28] In the case of $NbSe_2$, the distinct $\kappa_0(H)/T$

behavior was well explained by multiple superconducting gaps with different magnitudes.[27]

From Fig. 4, the field dependence of $\kappa_0(H)/T$ for $AuTe_2Se_{4/3}$ grows slightly faster than that of the dirty s-wave superconductor InBi and lower than that of the multiband s-wave superconductor $NbSe_2$. In fact, it almost overlaps that of $BaFe_{1.9}Ni_{0.1}As_2$. In $NbSe_2$, the gap on the Γ band is approximately one-third of the gap on the other two Fermi surfaces, and the magnetic field first suppresses the superconductivity on the Fermi surface with smaller gap,[27] thus $\kappa_0/T(H)$ increases much rapid at low field. The optimally electron-doped $BaFe_{1.9}Ni_{0.1}As_2$ has a slower field dependence of $\kappa_0(H)/T$ than $NbSe_2$.[32] Previously, it was explained by using the multiple superconducting gaps of its sister compound, the optimally electron-doped $BaFe_{1.85}Co_{0.15}As_2$, which has the average gap values $\Delta(0) = 6.6$ meV and 5.0 meV for hole and electron pockets, respectively.[33] This ratio of different gap magnitudes $R = 6.6/5.0 = 1.3$ is much smaller than that of $NbSe_2$ ($R \approx 3$). Due to the similarity between the $\kappa_0(H)/T$ of $AuTe_2Se_{4/3}$ and $BaFe_{1.9}Ni_{0.1}As_2$, $AuTe_2Se_{4/3}$ is likely also a multiband s-wave superconductor. Indeed, electronic structure calculations of $AuTe_2Se_{4/3}$ show there are four bands crossing the Fermi level along different directions in Brillouin zone, including three 3D bands and one quasi-1D band.[16] In this sense, the ratio of the magnitudes for different superconducting gaps in $AuTe_2Se_{4/3}$ should be around 1.3 as well.

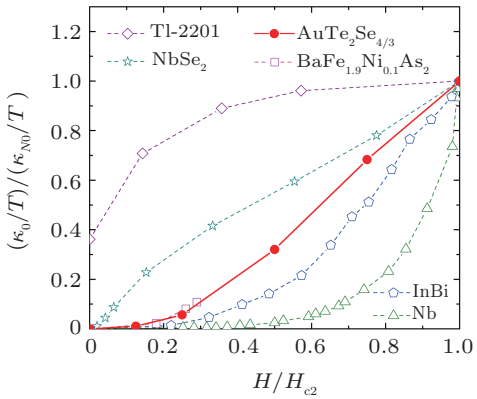


Fig. 4. (color online) Normalized residual linear term κ_0/T of $AuTe_2Se_{4/3}$ as a function of H/H_{c2}. For comparison, similar data are shown for the clean s-wave superconductor Nb,[30] the dirty s-wave superconducting alloy InBi,[31] the multiband s-wave superconductor $NbSe_2$,[27] and iron-based superconductor $BaFe_{1.9}Ni_{0.1}As_2$,[32] and an overdoped d-wave cuprate superconductor Tl-2201.[28]

So far, among all multi-band s-wave superconductors, only the iron-based superconductors are unconventional with the possible $s_{\pm}$-wave pairing.[34] Therefore, the multiple s-wave gap we observe in $AuTe_2Se_{4/3}$ indicates conventional superconductivity in it. This is reasonable, since unconventional superconductivity usually involves magnetism,[35] while $AuTe_2Se_{4/3}$ is nonmagnetic. As a new vdW quasi-2D superconductor, it will be interesting to fabricate $AuTe_2Se_{4/3}$ thin flakes to investigate whether its superconductivity can be enhanced by gating techniques, like in other quasi-2D compounds.[8,36–41]

4. Conclusion

In summary, the superconducting gap structure of the new gold-based quasi-2D superconductor $AuTe_2Se_{4/3}$ has been studied by the ultra-low temperature thermal conductivity measurements. A negligible κ_0/T in zero field and the field dependence of κ_0/T suggest multiple nodeless superconducting gaps. This is consistent with the band structure calculations which shows four Fermi surfaces in $AuTe_2Se_{4/3}$. To confirm those multiple gaps, further experiments like angle-resolved photoemission spectroscopy (ARPES) and scanning tunneling microscope (STM) are needed.

References

[1] Wang Q Y, Li Z, Zhang W H, Zhang Z C, Zhang J S, Li W, Ding H, Ou Y B, Deng P, Chang K, Wen J, Song C L, He K, Jia J F, Ji S H, Wang Y Y, Wang L L, Chen X, Ma X C and Xue Q K 2012 *Chin. Phys. Lett.* **29** 037402
[2] Xing Y, Zhang H M, Fu H L, Liu H, Sun Y, Peng J P, Wang F, Lin X, Ma X C, Xue Q K, Wang J and Xie X C 2015 *Science* **350** 542
[3] Saito Y, Nojima T and Iwasa Y 2016 *Nat. Rev. Mater.* **2** 16094
[4] Qin S, Kim J, Niu Q and Shih C K 2009 *Science* **324** 1314
[5] Zhang T, Cheng P, Li W J, Sun Y J, Wang G, Zhu X G, He K, Wang L L, Ma X C, Chen X, Wang Y Y, Liu Y, Lin H Q, Jia J F and Xue Q K 2010 *Nat. Phys.* **6** 104
[6] Reyren N, Thiel S, Caviglia A D, Kourkoutis L F, Hammerl G, Richter C, Schneider C W, Kopp T, Rüetschi A S, Jaccard D, Gabay M, Muller D A, Triscone J M and Mannhart J 2007 *Science* **317** 1196
[7] Gozar A, Logvenov G, Kourkoutis L F, Bollinger A T, Giannuzzi L A, Muller D A and Bozovic I 2008 *Nature* **455** 782
[8] Ye J T, Zhang Y J, Akashi R, Bahramy M S, Arita R and Iwasa Y 2012 *Science* **338** 1193
[9] Saito Y, Nakamura Y, Bahramy M S, Kohama Y, Ye J, Kasahara Y, Nakagawa Y, Onga M, Tokunaga M, Nojima T, Yanase Y and Iwasa Y 2015 *Nat. Phys.* **12** 144
[10] Cao Y, Fatemi V, Fang S, Watanabe K, Taniguchi T, Kaxiras E and Jarillo-Herrero P 2018 *Nature* **556** 43
[11] Cao Y, Fatemi V, Demir A, Fang S, Tomarken S L, Luo J Y, Sanchez-Yamagishi J D, Watanabe K, Taniguchi T, Kaxiras E, Ashoori R C and Jarillo-Herrero P 2018 *Nature* **556** 80
[12] Jiang D, Hu T, You L, Li Q, Li A, Wang H, Mu G, Chen Z, Zhang H, Yu G, Zhu J, Sun Q, Lin C, Xiao H, Xie X and Jiang M 2014 *Nat. Commun.* **5** 5708
[13] Xi X, Zhao L, Wang Z, Berger H, Forro L, Shan J and Mak K F 2015 *Nat. Nanotechnol.* **10** 765
[14] Staley N E, Wu J, Eklund P, Liu Y, Li L and Xu Z 2009 *Phys. Rev. B* **80** 184505
[15] Xi X, Wang Z, Zhao W, Park J H, Law K T, Berger H, Forro L, Shan J and Mak K F 2016 *Nat. Phys.* **12** 139
[16] Guo J G, Chen X, Jia X Y, Zhang Q H, Liu N, Lei H C, Li S Y, Gu L, Jin S F and Chen X L 2017 *Nat. Commun.* **8** 871
[17] Duwez P, Willens R H and Klement W 1960 *J. Appl. Phys.* **31** 1136
[18] Luo H and Klement W 1962 *J. Chem. Phys.* **36** 1870
[19] Tsuei C C and Newkirk L R 1969 *Phys. Rev.* **183** 619
[20] Gurevich A 2003 *Phys. Rev. B* **67** 184515
[21] Gurevich A 2007 *Physica C Supercond.* **456** 160
[22] Buzea C and Yamashita T 2001 *Supercond. Sci. Technol.* **14** R115
[23] Maple M B, Chen J W, Lambert S E, Fisk Z, Smith J L, Ott H R, Brooks J S and Naughton M J 1985 *Phys. Rev. Lett.* **54** 477
[24] Shakeripour H, Petrovic C and Taillefer L 2009 *New J. Phys.* **11** 055065

[25] Sutherland M, Hawthorn D G, Hill R W, Ronning F, Wakimoto S, Zhang H, Proust C, Boaknin E, Lupien C, Taillefer L, Liang R, Bonn D A, Hardy W N, Gagnon R, Hussey N E, Kimura T, Nohara M and Takagi H 2003 *Phys. Rev. B* **67** 174520
[26] Li S Y, Bonnemaison J B, Payeur A, Fournier P, Wang C H, Chen X H and Taillefer L 2008 *Phys. Rev. B* **77** 134501
[27] Boaknin E, Tanatar M A, Paglione J, Hawthorn D, Ronning F, Hill R W, Sutherland M, Taillefer L, Sonier J, Hayden S M and Brill J W 2003 *Phys. Rev. Lett.* **90** 117003
[28] Proust C, Boaknin E, Hill R W, Taillefer L and Mackenzie A P 2002 *Phys. Rev. Lett.* **89** 147003
[29] Suzuki M, Tanatar M A, Kikugawa N, Mao Z Q, Maeno Y and Ishiguro T 2002 *Phys. Rev. Lett.* **88** 227004
[30] Lowell J and Sousa J B 1970 *J. Low Temp. Phys.* **3** 65
[31] Willis J O and Ginsberg D M 1976 *Phys. Rev. B* **14** 1916
[32] Ding L, Dong J K, Zhou S Y, Guan T Y, Qiu X, Zhang C, Li L J, Lin X, Cao G H, Xu Z A and Li S Y 2009 *New J. Phys.* **11** 093018
[33] Terashima K, Sekiba Y, Bowen J H, Nakayama K, Kawahara T, Sato T, Richard P, Xu Y M, Li L J, Cao G H, Xu Z A, Ding H and Takahashi T 2009 *Proc. Natl. Acad. Sci.* **106** 7330
[34] Chen X H, Dai P C, Feng D L, Xiang T and Zhang F C 2014 *Nat. Sci. Rev.* **1** 371
[35] Norman M R 2011 *Science* **332** 196
[36] Ueno K, Shimotani H, Yuan H, Ye J, Kawasaki M and Iwasa Y 2014 *J. Phys. Soc. Jpn.* **83** 032001
[37] Saito Y, Kasahara Y, Ye J, Iwasa Y and Nojima T 2015 *Science* **125** 9440
[38] Shi W, Ye J, Zhang Y, Suzuki R, Yoshida M, Miyazaki J, Inoue N, Saito Y and Iwasa Y 2015 *Sci. Rep.* **5** 12534
[39] Lei B, Cui J H, Xiang Z J, Shang C, Wang N Z, Ye G J, Luo X G, Wu T, Sun Z and Chen X H 2016 *Phys. Rev. Lett.* **116** 077002
[40] Lei B, Wang N Z, Shang C, Meng F B, Ma L K, Luo X G, Wu T, Sun Z, Wang Y, Jiang Z, Mao B H, Liu Z, Yu Y J, Zhang Y B and Chen X H 2017 *Phys. Rev. B* **95** 020503
[41] Ying T P, Wang M X, Zhao Z Y, Zhang Z Z, Jia X Y, Li Y C, Lei B, Li Q, Yu Y, Cheng E J, An Z H, Zhang Y, Yang W, Chen X H and Li S Y 2018 arXiv: 1802.01484 [cond-mat]